Available online at www.sciencedirect.com
ScienceDirect
Proceedings of the Combustion Institute 000 (2018) 1–8
Proceedings of the Combustion Institute
www.elsevier.com/locate/proci

Role of radicals on MILD combustion inception

N.A.K. Doan*, N. Swaminathan

Department of Engineering, University of Cambridge, Trumpington Street, Cambridge CB2 1PZ, United Kingdom

Received 29 November 2017; accepted 6 July 2018
Available online xxx

Abstract

The criterion used to define MILD combustion in non-premixed condition is analysed using Direct Numerical Simulation (DNS) of MILD combustion of methane-diluted air established with internal exhaust gas recirculation. The simulations reveal multiple interacting reaction zones in MILD combustion which are extremely different from conventional combustion. Furthermore, DNS deduced S-curves highlight the role of chemically active species. Specifically, the temperature rise is accompanied with an increase in the scalar dissipation rate of mixture fraction, which is quite contrasting to the classical S-curve from the classical flame theories. This observation is explained on a physical basis.

Keywords: Direct Numerical Simulation (DNS); Exhaust Gas Recirculation (EGR); Moderate or Intense Low-oxygen Dilution (MILD); Flameless combustion; Ignition

1. Introduction

To mitigate the environmental impact of conventional combustion, alternative combustion concepts and technologies are explored constantly. Among these, Moderate or Intense Low-oxygen Dilution (MILD) combustion has been identified as a potential candidate offering more efficient, "silent" and cleaner combustion systems [1–3]. MILD combustion involves both preheating and dilution of reactant mixture with recirculated burnt products. As a result of this recirculation, which can be both external or internal to the combustion chamber, the oxygen content decreases drastically limiting the temperature rise and thus the NO_x production.

Due to these particular conditions involving exhaust gas recirculation (EGR) and highly preheated reactants, MILD combustion shows specific features such as the absence of a visible flame, heat release distributed over larger volumes and homogeneous temperature fields [4–6]. Furthermore, given the high reactants temperature and the presence of chemically active species in the recirculated exhaust gases, autoignition plays an important role in MILD combustion in addition to propagating flames [7–9].

Various definitions have been proposed to characterise MILD combustion in the past using classical combustion theories involving a single step irreversible reaction. The original definition used a Perfectly Stirred Reactor (PSR) as a representative canonical model [10]. This was motivated

* Corresponding author.
E-mail address: nakd2@cam.ac.uk (N.A.K. Doan).

https://doi.org/10.1016/j.proci.2018.07.038

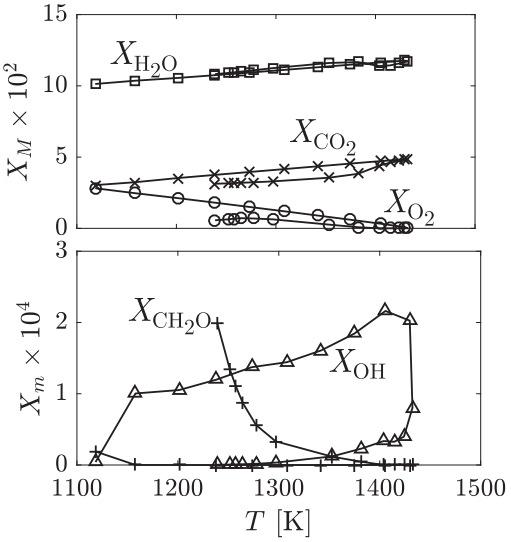

Fig. 1. Variation of major, X_M, and minor, X_m, species mole fractions with T for $0.1 \leq \phi \leq 5$ using the same oxidiser and fuel compositions as in [11,13].

by the homogeneous temperature in and the importance of ignition for MILD combustion, which was defined as a condition for which there were no critical (extinction or ignition) points when temperature is plotted against the residence time in the reactor [10]. This inference was made using a single irreversible reaction with large activation energy. The most widely used definition suggests [3] that MILD combustion occurs when $T_r > T_{\rm ign}$ and $\Delta T = (T_p - T_r) < T_{\rm ign}$, where T_r, T_p and $T_{\rm ign}$ are, respectively, the reactant, product and mixture autoignition temperatures. These definitions are appropriate for premixed scenarios but become ambiguous for non-premixed conditions since it does not involve scalar dissipation rate (SDR), N_Z, of the mixture fraction, Z. Thus, the definition [11] based on the analysis in [12], which extended the investigation in [10] to non-premixed situations by using a counterflow flame, was proposed to represent MILD combustion. A criteria, based on the S-curve for temperature at stoichiometric mixture fraction and the corresponding SDR, showing the absence of critical points was obtained, which is similar to that proposed in [10].

Although the theoretical analyses in [10] and [12] used a single reaction with no intermediate species, the elaborate simulations with complex chemical kinetics in [11] showed similar S-curve characteristics. However, it is important to note that there were no intermediate species present in the high temperature oxidiser stream (made of H_2O, CO_2, O_2 and N_2) for the opposed flow non-premixed flame. Figure 1 shows variation of product composition from the equivalent laminar premixed flames with T. These are computed using Cantera considering a premixed flame with an oxidiser at 1100 K with $X_{O_2} = 0.03$, $X_{CO_2} = 0.03$, $X_{H_2O} = 0.1$ and $X_{N_2} = 0.84$ and C_2H_4 as fuel for various equivalence ratio as in [11,13]. It is quite clear that these products contain non-negligible amount of intermediate species. Hence, in the oxidiser stream of a MILD combustor with internal EGR, one needs to allow for these intermediates to be present in the oxidiser stream, which would be akin to typical MILD combustion involving EGR. However, if one allows the intermediates in the oxidiser stream of the opposed-flow then the classical flame solution to obtain S-curves may not exist and thus the laminar configuration used in this previous definition of MILD combustion may not be entirely adequate as it cannot account for the effect of the radicals present in MILD mixture. This is because MILD combustion is shown to have premixed and non-premixed flames, and autoignition events entangled in space and time [7,9,14]. Thus, there are distinctive features of its own along with some characteristics of conventional flames in MILD combustion and hence, one needs to be cautious while defining it.

The objective of this work is to analyse these definitions, specifically the classical S-curve for non-premixed situations, using direct numerical simulation (DNS) data of MILD combustion [7] and subsequently assess if the definition based on laminar counterflow configuration [11] is suitable or not. Specifically, the role of chemically active radicals, i.e., radicals, such as CH_2O, OH or H, playing key-roles in the inception of MILD combustion, are studied. The previous definition of MILD combustion is briefly introduced in Section 2. The DNS data used are discussed in Section 3. Results are presented in Section 4 and conclusions are summarised in the final section.

2. S-curve for non-premixed combustion

The steady non-premixed flamelet equation was shown to be [11,12]:

$$\frac{N_{Z,st}}{N^0_{Z,st}}\theta_{st} = \dot{\omega}(\theta_{st}) \tag{1}$$

after making use of the Shvab–Zeldovich coupling function. The above equation is written for stoichiometric condition and thus the subscript st is used. The reference SDR is N^0_Z, $\theta_{\rm st} = (T_{\rm st} - T_{{\rm st},r})/(T_{{\rm st},p} - T_{{\rm st},r}) = (T_{\rm st} - T_{{\rm st},r})/\Delta T_{\rm st}$ and $\dot{\omega}$ is the normalised reaction rate for a one-step reaction, given by

$$\dot{\omega}(\theta_{st}) = {\rm Da}\exp(\beta_{ref} - \beta)\frac{(1-\alpha)(1-\theta_{\rm st})^2}{[1-\alpha(1-\theta_{\rm st})]\theta_{\rm st}} \times \exp\left(-\frac{\alpha\beta(1-\theta_{\rm st})}{1-\alpha(1-\theta_{\rm st})}\right) \tag{2}$$

Please cite this article as: N.A.K. Doan, N. Swaminathan, Role of radicals on MILD combustion inception, Proceedings of the Combustion Institute (2018), https://doi.org/10.1016/j.proci.2018.07.038

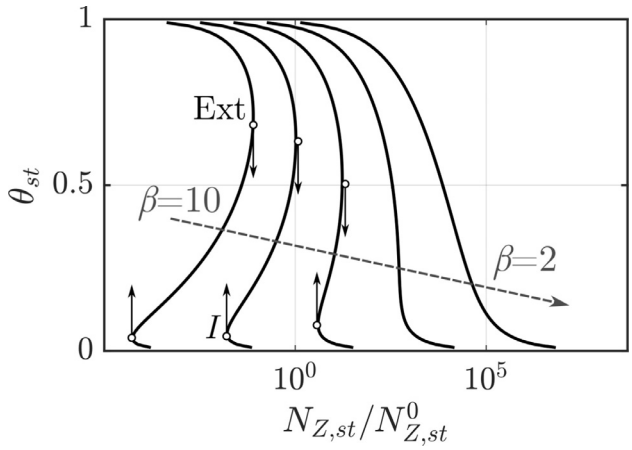

Fig. 2. S-curves with $\beta = 2$, 4, 6, 8 and 10, illustrating the conditions of non-premixed conventional and MILD combustion for Da = 100, $\alpha = 0.679$ and $\beta_{ref} = 8.03$ (as in [11,12]).

with Da as the Damköhler number, $\beta = E_{\text{eff}}/(RT_{\text{st},p})$ as the normalised activation temperature and $\alpha = \Delta T_{\text{st}}/T_{\text{st},p}$.

Figure 2 shows typical S-curves (indeed "Z"-curves, which become S-curves if $N^0_{Z,\text{st}}/N_{Z,\text{st}}$ is used) for various values of β obtained using Eqs. (1) and (2). In conventional combustion (curves with $\beta = 6$, 8, 10), ignition (a jump from low θ_{st} to high θ_{st}) occurs when $N_{Z,\text{st}}$ is decreased to reach a critical value, marked as I in the figure. If $N_{Z,\text{st}}$ is increased for a fully burning flame (the upper branch with $\theta_{\text{st}} = 1$), then extinction (Ext) occurs at another critical value as seen in Fig. 2. It should be noted that the branch between I and "Ext" points is unstable and there is no stable flame in that region. In the case of MILD combustion [11], the flame does not exhibit this ignition/extinction behaviour and there is a monotonic increase/decrease in temperature with N_Z as observed for the curves with $\beta = 2$ and 4 in Fig. 2.

The critical points are obtained using $dN_{Z,\text{st}}/d\theta_{\text{st}} = 0$ on Eq. (1), which gives $(\beta^2 + 6\beta + 1)\alpha^2 - (6\beta - 2)\alpha + 1 \leq 0$ for MILD combustion, monotonic variation from unburnt to burnt state, ie., absence of the critical points (extinction or ignition). Solving for α using this condition gives [11]:

$$\frac{\Delta T_{st}}{T_r} < (1 + \widehat{H}) f(\beta) \text{ with } f(\beta) = \frac{(6\beta - 2) \pm \sqrt{32\beta^2 - 48\beta}}{2(\beta^2 + 6\beta + 1)} \quad (3)$$

with $\widehat{H} = HY_{f,r}/(C_pT_r)$ as the normalised heating value of the fuel. The symbols $Y_{f,r}$ and C_p represent the fuel mass fraction and specific heat capacity at constant pressure respectively and H is the fuel heating value. It should be noted that in Eq. (3), only the largest value of $f(\beta)$ serves as a plausible root as the other root (negative sign) may be unphysical. The above discussion helps us to understand the various approximations invoked to define MILD combustion using classical analysis. The adequacy of this analysis and the ensuing definition, given the insights gathered from the DNS [7], for MILD combustion will be discussed in Section 4.

3. DNS of MILD combustion

Previous DNS of MILD combustion considered either an auto-igniting mixing layer between methane and hot diluted coflow [15,16] or premixed MILD combustion with internal EGR [9,14,17]. In this work, non premixed MILD combustion with internal EGR is considered. Indeed, typical MILD combustion involves high momentum fuel and air jets issuing into a stream of recirculating exhaust gases. This results in an inhomogeneous mixture of air, fuel and exhaust gases in burnt, partially burnt and unburnt states. DNS of a typical MILD combustion system with EGR is beyond the reach of current computational capabilities and a simplified two-stage approach was used in earlier studies [7,14]. The exact methodology is detailed in [7] for non-premixed MILD combustion and a brief description is given below.

The DNS considered MILD combustion of methane with air diluted using exhaust gases at atmospheric pressure in a cubic domain. In a first stage, a turbulence field with the desired attributes such as the integral lengthscale and rms velocity fluctuations is generated using a prescribed turbulent kinetic energy spectrum as described in [18]. Then, in a second stage, a preprocessed field containing a mixture of fresh ($c = 0$) and exhaust gases with mixture fraction variation ($0 \leq Z \leq 0.1$) is constructed, where c is a reaction progress variable. This is achieved by generating an initial c and Z

Please cite this article as: N.A.K. Doan, N. Swaminathan, Role of radicals on MILD combustion inception, Proceedings of the Combustion Institute (2018), https://doi.org/10.1016/j.proci.2018.07.038

Table 1
Oxidiser composition for the initial laminar MILD mixture.

Case	$X_{O_2,ox}$	$X_{H_2O,ox}$	$X_{CO_2,ox}$	$X_{N_2,ox}$
AZ1-2	0.035	0.134	0.067	0.764
BZ1	0.020	0.146	0.073	0.761

fields with specified means, $\langle c \rangle$ and $\langle Z \rangle$, and lengthscales, ℓ_c and ℓ_Z using the scalar-energy spectrum method described in [19]. Then, the species mass fractions, Y_i, from laminar premixed flames under MILD conditions of varying Z are mapped onto c and Z fields as explained in [7]. These laminar premixed flames come from a library of pre-computed laminar flames obtained by varying the mixture fraction and oxidiser dilution level. The composition of the oxidiser stream for these laminar flames is listed in Table 1 for the cases considered while the fuel stream has pure methane. These scalars are then allowed to evolve in a periodic domain with the turbulence field previously generated for about one large eddy turnover time without any chemical reactions, which yields partially premixed mixture containing fresh, partially burnt and exhaust gases. This mimicks the exhaust gas recirculation of MILD combustion and the duration of this mixing is much lower than the autoignition delay for the chosen mixtures. These fields serve as the initial and inflowing conditions for the MILD combustion DNS in the second stage. Elaborate details of these procedures are given in [7].

Laminar premixed flames for various equivalence ratios have been used to construct the initial scalar fields. Other configurations such as a PSR or counterflow flame could also have been used but it was observed that the variations of Y_i with Z and c were similar among all of these configurations under fully reacting conditions [7] and thus, a specific choice would not unduly influence the results reported here. Furthermore, the characteristics chemical timescales, the autoignition delay time for the PSR and flame time, δ_{th}/s_L, for the laminar flame, are larger than the initial eddy-turnover time when simulating the mixing stage described above [7].

Three cases, detailed in Tables 1 and 2, are considered. The base case, AZ1, and AZ2 uses the same oxidiser with 3.5% by volume of O_2 while the case BZ1 considers more diluted conditions (2% of O_2) as noted in Table 1. The effect of the lengthscale ratio, ℓ_c/ℓ_Z, on MILD combustion can be investigated by comparing AZ1 and AZ2. The case of $\ell_c/\ell_Z > 1$ is not considered here because chemical lengthscales such as flame thickness or ignition kernel size at large T_r (1500 K here), are typically smaller than the mixing (mixture fraction) scale. All cases have similar turbulence with an integral length scale of $\Lambda_0 \approx 1.42$ mm and root-mean square value of $u' \approx 16.66$ m/s for the velocity fluctuations. The corresponding turbulence and Taylor microscale Reynolds numbers are $\mathrm{Re}_t \approx 96$ and $\mathrm{Re}_\lambda \approx 34.73$, respectively.

The numerical domain is a cube of size $L_x \times L_y \times L_z = 10 \times 10 \times 10\,\mathrm{mm}^3$ with inflow and non-reflecting outflow boundary conditions specified using NSCBC in the x-direction, with the inlet located at $x = 0$ and the outlet at $x = L_x$, and periodic conditions in the transverse, y and z, directions. The domain is discretised using $512 \times 512 \times 512$ uniformly distributed grid points to resolve all chemical and turbulence lengthscales [7]. The chemical mechanism used is a combination of the Smooke and Giovangigli [20] and KEE-58 [21] mechanisms for methane-air combustion, and OH^* chemistry from [22]. This mechanism, listed in [7], involves 19 species and 58 reactions, and balances appropriately the accuracy and computational cost by giving a good agreement for laminar flame speed and ignition delay as discussed in [7].

A well established code, SENGA2, which solves fully compressible conservation equations for mass, momentum, internal energy and species mass fractions, Y_i, is used. These equations are discretised in space using a tenth order central difference scheme and a third-order low storage Runge–Kutta scheme for time integration. The transport and thermo-chemical properties are temperature dependent with non-unity constant Lewis numbers. Each case is run for 1.5 flow-through time, $\tau_f = L_x/U_{in}$ where $U_{in} = 20$ m/s is the inflowing velocity. To ensure that the transients from the initial conditions have left the domain, statistics are only taken after the first flow-through time and 50 snapshots are taken for each case for detailed analysis.

4. Results and discussions

4.1. DNS results

Figure 3 shows a typical iso-surface of normalised heat release rate $\dot{Q}^+ = \dot{Q}\delta_{\mathrm{th}}/(\rho_r s_L C_P(T_p - T_r))$ for $\dot{Q}^+ = 2.0$ for cases AZ1 and BZ1. The

Table 2
DNS initial conditions.

Case	Λ_0/ℓ_Z	$\langle X_{O_2} \rangle$	$X_{O_2}^{\max}$	ℓ_c/ℓ_Z	$\langle Z \rangle$	Z_{st}	σ_Z^2	$\langle c \rangle$	σ_c^2
AZ1	0.60	0.0270	0.035	0.77	0.008	0.010	0.00007	0.56	0.068
AZ2	0.79	0.0285	0.035	0.99	0.008	0.010	0.00011	0.56	0.078
BZ1	0.60	0.0160	0.020	0.77	0.0046	0.0058	0.00003	0.56	0.068

Please cite this article as: N.A.K. Doan, N. Swaminathan, Role of radicals on MILD combustion inception, Proceedings of the Combustion Institute (2018), https://doi.org/10.1016/j.proci.2018.07.038

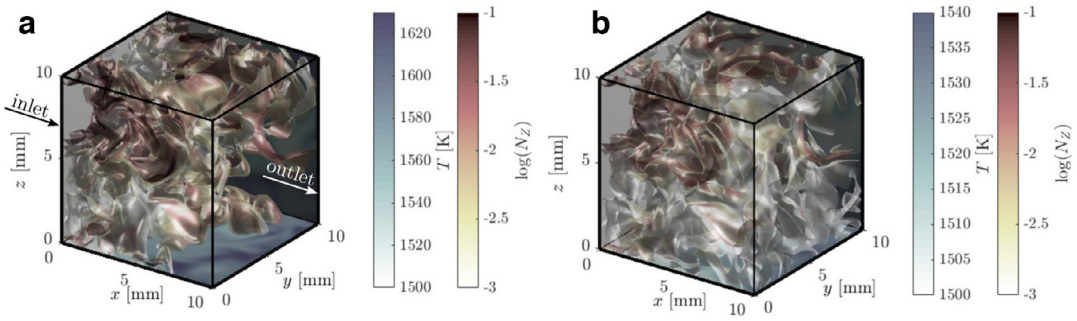

Fig. 3. Typical iso-surfaces of normalised heat release rate $\dot{Q}^+ = 2.0$ at $t = 1.5\tau_f$ for cases (a) AZ1 and (b) BZ1, coloured by $\log(N_Z)$. The temperature field is shown on the bottom and side surfaces.

normalisation is done using the thermo-chemical quantities for the local mixture fraction. The iso-surface is coloured by $\log(N_Z)$ and the temperature field is shown on the bottom and side surfaces. It is observed that the increase in temperature is about 150 K for case AZ1. The reaction zones are extremely convoluted and multiply connected. The multiply connected reaction zones lead inevitably to their interactions which result in their apparent broadening [7]. Compared to case AZ1, the case BZ1 shows increased volumetrically distributed reaction with broader reaction zones. Furthermore, N_Z varies over several orders of magnitude and it is also apparent that reactions (and ignition) occur in regions of high (compared to the mean) SDR. The absence of predominantly thin regions of large heat release rate in a narrow portion of the domain with a small overall temperature rise suggests that the combustion is occurring in MILD condition.

4.2. Assessment of MILD combustion definition

From the DNS data, the S-curve, similar to those presented in Fig. 2, can be constructed by extracting N_Z and $\theta = (T - T_r)/(T_{\max} - T_r)$. There are two ways to plot this result, one is to consider the entire domain and construct:

$$\langle N_Z|\theta\rangle = \int N_Z\, p(N_Z|\theta)\; dN_Z. \tag{4}$$

The other way is to consider the conditionally averaged quantities along the stoichiometric mixture fraction and this is given by

$$\langle N_Z|\theta_{st}, Z = Z_{st}\rangle = \int N_Z\, p(N_Z|\theta_{st}, Z_{st})\; dN_Z \tag{5}$$

The conditional probability density function (pdf) of N_Z conditioned on θ is $p(N_Z|\theta)$. The doubly conditioned pdf of N_Z on θ and $Z = Z_{\rm st}$ is $p(N_Z|\theta, Z_{\rm st})$. These pdfs are constructed using samples collected over the entire sampling time. In the expression for θ, $T_r = 1500$ K is the unburnt temperature and $T_{\max}$ is the maximum temperature either for stoichiometric mixture or for the entire domain depending on if Eqs. (5) or (4) is used.

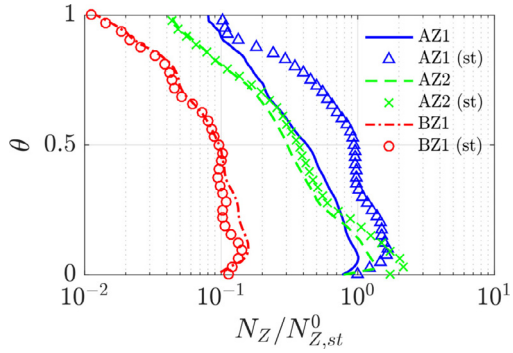

Fig. 4. Variation of normalised temperature with SDR. This variation for $Z_{\rm st}$ is also shown.

The results are plotted in Fig. 4 for all cases, where N_Z for each case is normalised by $N^0_{Z,\rm st}$ defined as $\langle N_Z|\theta = 0, Z_{\rm st}\rangle$ computed for case AZ1. The DNS results show a different behaviour compared to the laminar cases depicted in Fig. 2. Specifically, θ increases with $N_Z/N^0_{Z,\rm st}$ near $\theta = 0$, which is the opposite of the behaviour in Fig. 2. For larger θ, the increase in θ is accompanied by a decrease in N_Z which is similar to the classical S-curve. These observations hold for both stoichiometric (symbols) or entire (lines) mixture as shown in Fig. 4. The difference between the entire and stoichiometric mixtures in case AZ1 is because of the difference in the mixture fraction distribution and its lengthscale which leads to different SDR for these mixtures but both the entire and stoichiometric mixtures exhibit this particular behaviour during inception. Furthermore, this behaviour was also observed when considering the pdf constructed from just an instantaneous snapshot (not shown here) and thus the observations made using Fig. 4 hold both statistically and instantaneously for MILD combustion. The constrasting

Please cite this article as: N.A.K. Doan, N. Swaminathan, Role of radicals on MILD combustion inception, Proceedings of the Combustion Institute (2018), https://doi.org/10.1016/j.proci.2018.07.038

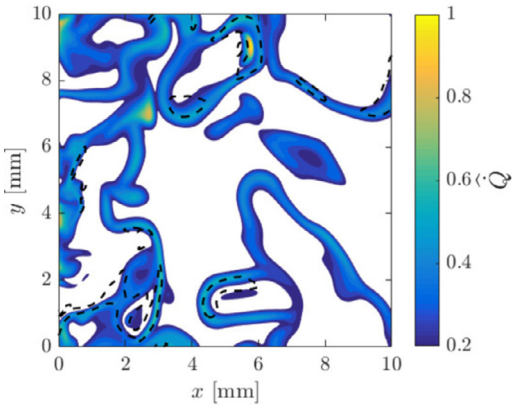

Fig. 5. Typical variation of $\widehat{Q}$ in the mid x–y plane for case AZ1 at $t = \tau_f$. Dashed black lines enclose regions with $\widehat{N}_Z > 0.2$.

behaviour near $\theta = 0$ (inception of combustion) is quite intriguing and is explored further below.

Figure 5 depicts regions of heat release rate normalised using the maximum value in the mid x–y plane shown. The top 80% is shown to highlight regions with large heat release rate and the white regions have $\widehat{Q} < 0.2$. The dashed black lines show contours of $\widehat{N}_Z = N_Z / \max(N_Z) = 0.2$. Here and in the following discussion, quantities with a hat imply that they are normalised using the maximum value observed in the plane chosen for the analysis. This threshold value of 0.2 is used to focus on region of high SDR and large heat release rate. It is quite clear that the regions with large heat release rate and $\widehat{N}_Z$ values overlap, which is specifically so in the upstream part of the computational domain. This behaviour gives the lower branch (with both θ and $N_Z/N^0_{Z,\mathrm{st}}$ increasing) of the DNS S-curve shown in Fig. 4. Although a single plane at a particular time is shown in Fig. 5 for case AZ1, similar situations were also found for cases AZ2 and BZ1 (not shown here) and the result in Fig. 4 demonstrates that such a behaviour occurs in other planes and at other times since the data collected over the entire sampling period is used for Fig. 4.

The reason behind this increase in θ with an increase in N_Z during the inception stems from the nature of MILD combustion with internal EGR. Indeed, the mixture for MILD combustion with internal EGR contains fuel, air and combustion products with chemically active radicals as established in Fig. 1. The radicals such as CH_2O, OH and H, play a key role in initiating the combustion reactions. This is demonstrated in Fig. 6 showing specifically CH_2O and OH mass fractions fields normalised using their respective maximum values

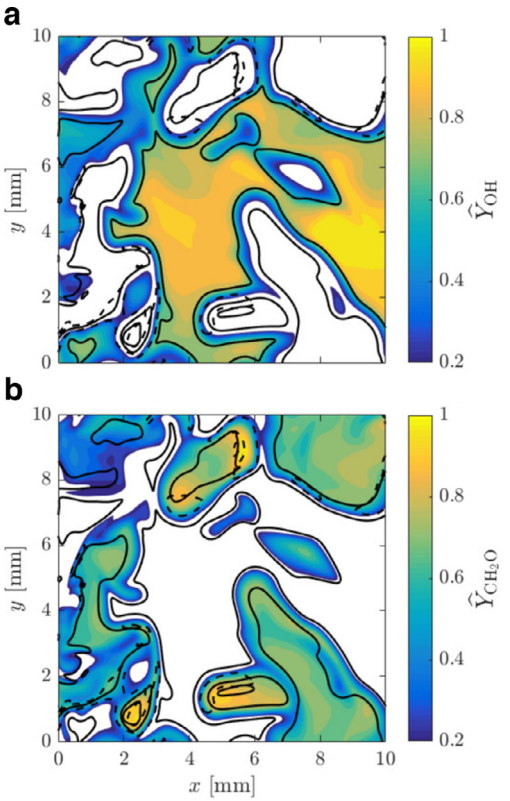

Fig. 6. Variation of (a) $\widehat{Y}_{OH}$ and (b) $\widehat{Y}_{CH_2O}$ in the mid x–y plane for case AZ1 at $t = \tau_f$. Isolines of $\widehat{Q} = 0.2$ (full black lines) and $\widehat{N}_Z = 0.2$ (dashed) are also shown.

observed in the plane shown. The radicals present in the recirculated hot gases give non-zero (indeed quite high) values of $\widehat{Y}_{CH_2O}$ and $\widehat{Y}_{OH}$, which are of interest to understand the inception of MILD combustion. The relatively larger values seen in Fig. 6 for the middle and downstream parts of the domain are because of the combustion occurring in the domain. A closer scrutiny of the results in Fig. 6 shows that the high SDR are occurring in regions with overlapping $\widehat{Y}_{OH}$ and $\widehat{Y}_{CH_2O}$. This is particularly so in the upstream 30% of the computational domain, where the MILD combustion begins. Hence, it is quite clear that the radicals play a vital role in the inception of MILD combustion which gives a quite different behaviour for the lower branch of the S-curve compared to the classical behaviour as seen in Fig. 4.

The role of these radicals on the inception of MILD combustion, OH in particular, is further explored by considering a quantity $\Delta Y_{OH} = Y_{OH} - Y^c_{OH}$, where Y^c_{OH} is the local value of the *incoming* OH mass fraction where there is no combustion. This quantity is obtained by performing a DNS with the same initial and inflowing fields (species

Please cite this article as: N.A.K. Doan, N. Swaminathan, Role of radicals on MILD combustion inception, Proceedings of the Combustion Institute (2018), https://doi.org/10.1016/j.proci.2018.07.038

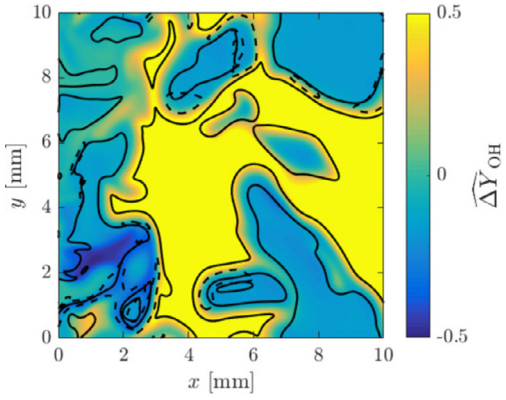

Fig. 7. Variation of $\widehat{\Delta Y}_{OH}$ in the mid x–y plane for case AZ1 at $t = \tau_f$. Isolines of $\widehat{Q} = 0.2$ (full black lines) and $\widehat{N}_Z = 0.2$ (dashed) are also shown.

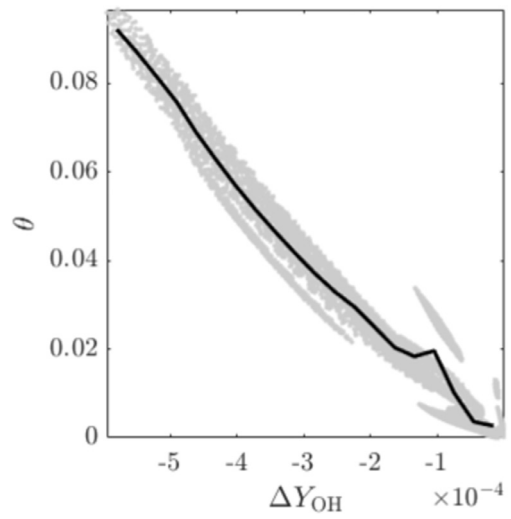

Fig. 8. Variation of ΔY_{OH} with θ for points with $\widehat{N}_Z > 0.2$ and axial locations $0 \le x/L_x \le 0.05$ for case AZ1 at $t = \tau_f$. The corresponding conditional average $\langle\theta|\Delta Y_{OH}\rangle$ is plotted as full black line.

and velocities) as the present MILD combustion DNS but by removing all the chemical reactions. One, then, obtains the purely convective-diffusive evolution for the species inside the computational domain with the same turbulence field. Since the temperature rise in the MILD combustion DNS is moderate, only few tens of Kelvin, the velocity fields in this and the convective-diffusive cases remain similar, especially in regions close to the inlet. A comparison of the species mass fractions from the combustion DNS to those from the convective-diffusive case allows one to understand the local influence of combustion on these species, at a given time and location. Hence, $\Delta Y_{OH} > 0$ implies that OH is produced locally by combustion since the local Y_{OH} is larger than Y^c_{OH}. The values of ΔY_{OH} normalised by its maximum value in the plane shown is plotted in Fig. 7 and it is seen that close to the inlet, the normalised value, $\widehat{\Delta Y}_{OH}$, is mostly negative. This indicates that the incoming OH is consumed by chemical reactions, i.e., $Y_{OH} < Y^c_{OH}$. Thus, the OH in the incoming recirculated exhaust gases is consumed and acts as a precursor for initiating ignition and heat release – inception of MILD combustion.

The importance of the incoming radicals is even more apparent if one cross-plots ΔY_{OH} with normalised temperature θ. This is shown in Fig. 8 as a scatter plot for regions with $\widehat{N}_Z = N_Z/\max(N_Z) \ge 0.2$ with $\max(N_Z)$ as the maximum for the chosen timestep. The samples are collected from the upstream portion of the domain, $0 \le x/L_x \le L_2 = 0.05$, since the focus is on the inception of MILD combustion. It is clear that there is a strong correlation between the temperature increase and the consumption of incoming OH. This further indicates that the inflowing radicals, here OH, play a key-role in the inception of MILD combustion, which is absent in the classical S-curve. This result was observed not to be strongly sensitive to L_2 up to $L_2 \approx 0.1$. Furthermore, this result was also observed not to be unduly influenced by the choice of the threshold for $\widehat{N}_Z$ (not shown here). Similar behaviours are observed for the cases AZ2 and BZ1. These results imply that the MILD combustion inception is driven by chemical kinetics initiated by the radicals present in the stream. As a result of this, in the early stage of the domain, an increase in N_Z implies increased small-scale mixing between neighbouring mixtures containing differing levels of radicals. This increased mixing promotes reactivity leading to an increase in θ.

From the analysis presented here using DNS of MILD combustion with internal EGR, it is clear that the past definitions of MILD combustion deduced using one-step chemistry in simplified configurations present various shortcomings. In particular, while the present DNSs also show a smooth ignition and a progressive increase in temperature, these definitions do not include the important role played by radicals in the inception of MILD combustion while over-emphasizing the importance of N_Z. Indeed, a one-step chemistry solely characterised by an activation energy cannot account for the presence of radicals on the reaction. However, these radicals in the incoming stream play a major role in initiating and sustaining combustion as has been noted in [1]. Furthermore, the preferential diffusion has been shown to be important in the past [16] and thus the unity Lewis number assumed in the earlier analysis may have to be revisited for MILD combustion.

Please cite this article as: N.A.K. Doan, N. Swaminathan, Role of radicals on MILD combustion inception, Proceedings of the Combustion Institute (2018), https://doi.org/10.1016/j.proci.2018.07.038

5. Conclusions

DNS of MILD combustion with internal EGR involving inhomogeneous mixture fraction have been analysed to study the inception of MILD combustion. It is shown that the S-curve deduced from the DNS data presents a unique and contrasting behaviour in the inception phase (lower branch) compared to the classical case. Indeed, there is an increase in θ with an increase in SDR which is the opposite of the classical S-curve. The classical behaviour of θ increasing with decreasing SDR is observed for higher values of θ. The contrasting behaviour in the inception phase is because of the chemically active radicals present in the incoming stream. These results highlight a need to revisit the definitions of MILD combustion specifically when there is EGR which is quite typical of MILD combustion applications. Indeed, previous definitions of MILD combustion [10,11] do not show this behaviour as they do not account for the effect of radicals and intermediate species. It should, however, be noted that the definition proposed by Cavaliere and De Joannon [3] seems to be adequate, as this criterion does not make any assumptions as to how the temperature rise occurs and only uses the initial and final temperatures. Hence, further investigations are required to improve our understanding of MILD combustion that depicts their unique attributes while sharing some common features of classical combustion [7,9]. Modelling these processes is quite challenging and will be addressed in future studies.

Acknowledgements

N.A.K.D. acknowledges the financial support of the Qualcomm European Research Studentship Fund in Technology. This work used the ARCHER UK National Supercomputing Service (http://www.archer.ac.uk) using computing time provided by EPSRC under the RAP project number e419 and the UKCTRF (e305).

References

[1] J.A. Wünning, J.G. Wünning, *Prog. Energy Combust. Sci.* 23 (1997) 81–94.
[2] M. Katsuki, T. Hasegawa, *Symp. Combust.* 27 (1998) 3135–3146.
[3] A. Cavaliere, M. de Joannon, *Prog. Energy Combust. Sci.* 30 (2004) 329–366.
[4] I.B. Ozdemir, N. Peters, *Exp. Fluids* 30 (2001) 683–695.
[5] M. de Joannon, A. Saponaro, A. Cavaliere, *Proc. Combust. Inst.* 28 (2000) 1639–1646.
[6] G. Sorrentino, P. Sabia, M. de Joannon, A. Cavaliere, R. Ragucci, *Flow, Turbul. Combust.* 96 (2016) 449–468.
[7] N.A.K. Doan, N. Swaminathan, Y. Minamoto, *Combust. Flame* 189 (2018) 173–189.
[8] P. Sabia, G. Sorrentino, A. Chinnici, A. Cavaliere, R. Ragucci, *Energy & Fuels* 29 (2015) 1978–1986.
[9] Y. Minamoto, N. Swaminathan, *Combust. Flame* 161 (2014) 1063–1075.
[10] M. Oberlack, R. Arlitt, N. Peters, *Combust. Theory Model.* 4 (2000) 495–509.
[11] M.J. Evans, P.R. Medwell, H. Wu, A. Stagni, M. Ihme, *Proc. Combust. Inst.* 36 (2017) 4297–4304.
[12] H. Pitsch, S. Fedotov, *Combust. Theory Model.* 5 (2001) 41–57.
[13] P.R. Medwell, P.A.M. Kalt, B.B. Dally, *Combust. Flame* 152 (2008) 100–113.
[14] Y. Minamoto, N. Swaminathan, R.S. Cant, T. Leung, *Combust. Sci. Technol.* 186 (2014) 1075–1096.
[15] J.A. van Oijen, *Proc. Combust. Inst.* 34 (2013) 1163–1171.
[16] M.U. Göktolga, J.A. van Oijen, L.P.H. de Goey, *Fuel* 159 (2015) 784–795.
[17] Y. Minamoto, N. Swaminathan, R.S. Cant, T. Leung, *Combust. Flame* 161 (2014) 2801–2814.
[18] R.S. Rogallo, *Nasa Tech. Memo.* (1981) 93.
[19] V. Eswaran, S.B. Pope, *Comput. Fluids* 16 (1988) 257–278.
[20] M.D. Smooke, V. Giovangigli, M.D. Smooke, in: Lecture Notes in Physics, 384, Springer, Berlin, Heidelberg, 1991, pp. 1–28.
[21] R.W. Bilger, S. Starner, R.J. Kee, *Combust. Flame* 80 (1990) 135–149.
[22] T. Kathrotia, U. Riedel, A. Seipel, K. Moshammer, A. Brockhinke, *Appl. Phys. B Lasers Opt.* 107 (2012) 571–584.

Please cite this article as: N.A.K. Doan, N. Swaminathan, Role of radicals on MILD combustion inception, Proceedings of the Combustion Institute (2018), https://doi.org/10.1016/j.proci.2018.07.038